Journal of Science and Transport Technology
Journal homepage: https://jstt.vn/index.php/en

Metaheuristic-Enhanced Machine Learning for Accurate Shear Strength Assessment of RC Deep Beams

Dang Khoa Do[1], Manh Ha-Nguyen[2], Thi Trang Pham[3], Thuy-Anh Nguyen[4]*
[1]The University of Sydney, NSW 2006, Australia; email: dado0559@uni.sydney.edu.au
[2]University of Transport Technology, Hanoi 100000, Vietnam; email: hanm@utt.edu.vn
[3] The University of Da Nang - University of Science and Technology, Da Nang 550000, Vietnam; email: pttrang@dut.udn.vn
[4]Research group on Industry 4.0 in Transportation (I4T group), University of Transport Technology, Trieu Khuc, Thanh Liet, Hanoi 100000, Vietnam; email: anhnt@utt.edu.vn

Article info
Type of article:
Original research paper

DOI:
https://doi.org/10.58845/jstt.utt.2025.en.5.4.13-30

***Corresponding author:**
Email address:
anhnt@utt.edu.vn

Received: 31/03/2025
Received in Revised Form: 18/10/2025
Accepted: 03/11/2025

Abstract: Extensive testing required by traditional structural engineering methods can be time-consuming and costly due to the complexity of the procedures involved. This work presents a novel machine learning approach for predicting the shear strength of reinforced concrete (RC) deep beams. It employs a Gradient Boosting (GB) algorithm, optimized using metaheuristic techniques, specifically the Golden Jackal Optimization (GJO) and Honey Badger Algorithm (HBA). To develop this approach, a comprehensive dataset of 314 experimentally tested RC deep beams with web openings was compiled from peer-reviewed literature. The dataset includes key features governing the shear strength. The GB model's hyperparameters were fine-tuned using GJO and HBA, with the GJO-optimized model (GB_06) showing superior performance. It achieved a coefficient of determination (R^2) of 0.9664 and a root mean squared error (RMSE) of 70.258 kN on the test dataset. Feature importance analysis using SHAP values identified the shear span-to-depth ratio, horizontal web reinforcement ratio, and vertical web reinforcement ratio as the key factors influencing shear strength. The proposed model offers significant improvements in accuracy and reliability, providing structural engineers with an efficient tool for design optimization and safety assessment of RC deep beams.

Keywords: shear strength, Gradient Boosting, machine learning, SHAP analysis.

1. Introduction

Reinforced concrete (RC) deep beams with web openings are critical structural elements in buildings, bridges, and various infrastructure projects. Unlike slender beams, deep beams are characterized by their low shear span-to-depth ratio, which results in significant shear deformations and a reliance on arch action for load transfer rather than conventional flexural behavior [1]. In contemporary structural design, web

openings are often integrated into RC deep beams to accommodate services like ventilation ducts, utility pipes, and electrical conduits [2, 3]. However, the inclusion of these openings disrupts the natural load path, induces stress concentrations at the corners of the openings, and alters the internal force distribution. These disruptions lead to a reduction in shear strength and changes to failure mechanisms [4–6]. The shear capacity of RC deep beams with web openings is influenced by a complex interplay of parameters, including the size, shape, and location of the openings; concrete compressive strength (CS); longitudinal and web reinforcement ratios; and the shear span-to-depth ratio. Recent experimental studies, such as Al-Enezi et al. [6], have further highlighted the impact of these parameters on ultra-high-performance fiber-reinforced concrete (UHPFRC) deep beams with web openings, emphasizing the need for precise predictive models to account for material and geometric variability. Given these complexities, accurate prediction of the shear strength is essential for ensuring structural safety and optimizing design efficiency.

Conventional methods for predicting the shear strength of RC deep beams, such as those outlined in design codes like [7] and AS3600-2018 [8], typically rely on empirical formulas or simplified analytical models, including the strut-and-tie method. While these approaches are effective for solid deep beams, their applicability decreases when web openings are introduced. Openings disrupt the assumed load paths, leading to stress concentrations and altered force distributions, which render traditional models either overly conservative or inaccurate. Experimental studies have sought to address these limitations. For instance, Yang et al. [9] applied upper-bound plasticity theory to investigate shear failure mechanisms in RC deep beams with openings, identifying distinct failure zones and highlighting the effects of opening size and inclined reinforcement on shear capacity. Similarly, Ashour and Yang [10] examined the influence of shear span-to-depth ratio and opening location, proposing modifications to traditional strut-and-tie models. Kong et al. [11] conducted experiments on 32 RC deep beams with openings to validate their predictive equation for shear strength; however, their model overestimated capacity when the yield line angle was less than 30°. Kubik's proposed equation [12] was limited to cases where openings intersected the load path, while Tan et al.'s method [13] failed to incorporate critical parameters such as shear span-to-depth ratio and reinforcement ratios. Despite their contributions, experimental investigations remain constrained by their time-consuming and costly nature, as well as their limited exploration of design parameters. These challenges emphasize the need for more reliable and generalized approaches that can accurately predict the shear strength of RC deep beams with web openings across a broader range of conditions.

Recent advancements in machine learning (ML) offer a promising alternative for addressing the challenges in civil engineering, material sciences [14, 15], construction management [16], especially structural engineering [17], and problems related to predicting the shear strength of RC deep beams. Unlike traditional methods, ML models can capture complex nonlinear relationships and interactions between parameters without relying on explicit physical assumptions. This capability makes them particularly suitable for analyzing the intricate behavior of RC beams with web openings. A study by Saleh et al. [18] demonstrated the potential of AI-based approaches by utilizing a hybrid dataset comprising experimental results and finite element (FE) simulations to estimate the shear capacity of RC deep beams. Their investigation tested several ML models, including Artificial Neural Networks (ANN), Gradient Boosting (GB), and ensemble techniques. Among these, the stacking ensemble model achieved a coefficient of determination (R^2) of 0.996, highlighting its ability to accurately capture nonlinear dependencies in the data. However, the

utilized dataset exhibited a significant imbalance, with 179 experimentally tested beams compared to 5032 FE-generated samples—approximately 30 times more FE data than experimental data. This reliance on FE simulations introduces uncertainties due to assumptions about boundary conditions, material properties, and mesh sensitivity, which may not fully align with experimental observations. Consequently, while ML models trained on such hybrid datasets demonstrate high predictive accuracy, their generalizability to practical engineering applications depends heavily on the reliability of the underlying FE simulations [19, 20]. Other studies have also explored ML techniques for predicting shear strength in RC deep beams. For instance, CatBoost models optimized through Bayesian techniques have shown high accuracy and reliability compared to traditional mechanics-based models in Megahed et al. [19]. The authors further demonstrated the efficacy of multiple ML models, including CatBoost and XGBoost, achieving robust shear strength predictions for RC deep beams using a comprehensive dataset of 840 samples. Augustino [20] employed ANN alongside finite element modeling to predict shear performance in deep beams with openings reinforced with waste tire steel fibers, highlighting the potential of ML for sustainable structural design. Similarly, parametric studies using SHAP analysis have identified critical factors such as shear span-to-depth ratio and reinforcement ratios as key contributors to shear strength predictions [21]. While significant progress has been achieved, challenges remain in bridging the gap between theoretical predictions and practical design applications. Many ML models are considered "black-boxes", thus limiting interpretability and hindering their adoption in engineering practice. Overall, while AI and ML approaches offer transformative potential for predicting shear strength in RC deep beams with web openings, their practical application requires careful consideration of data quality, model interpretability, and alignment with real-world structural behavior.

This research introduces a novel methodology employing the GB algorithm, a ML technique chosen for its capability to model complex nonlinear relationships, mitigate overfitting, and deliver robust predictions. To enhance its performance, metaheuristic optimization methods, namely Golden Jackal Optimization (GJO) and Honey Badger Algorithm (HBA), are utilized for hyperparameter tuning, ensuring improved prediction accuracy and computational efficiency. This approach addresses the limitations of previous studies by relying exclusively on experimental data, avoiding the uncertainties associated with FE-simulated samples. The dataset comprises 314 experimentally tested RC deep beams, sourced from peer-reviewed publications, spanning a wide range of design parameters. The exclusive use of experimental data ensures that the ML model is trained on unbiased and validated information, enhancing its reliability and applicability to practical engineering scenarios. By eliminating reliance on numerically generated data, this study aims to provide a shear strength prediction model that is both experimentally grounded and suitable for civil engineering applications.

2. RC deep beams dataset

To develop an accurate and robust predictive model for the shear strength of RC deep beams using the GB algorithm combined with metaheuristic optimization techniques, a comprehensive and reliable dataset is essential. This study utilizes a database comprising 314 experimentally tested RC deep beams with web openings, sourced from peer-reviewed journal publications [6, 22–38]. Each sample represents an individual beam, characterized by a range of material and geometric parameters that influence shear capacity.

The material parameters include concrete CS, reinforcement yield strength, and reinforcement content. Geometric parameters encompass factors such as cross-sectional dimensions, shear span-to-depth ratio, and the

size and location of web openings (Fig. 1). To systematically analyze the influence of these parameters on shear strength, nine input variables were selected: concrete CS, shear span-to-depth ratio, opening size ratios (a_x/a, a_y/a), opening location ratios (X_0/a, Y_0/H), reinforcement yield strength, and horizontal and vertical web reinforcement ratios. The statistical characteristics of these input and output parameters are summarized in Table 1, including metrics such as mean, standard deviation (Std), minimum (Min), maximum (Max), and quartile values (Q25, Q50, Q75). This dataset ensures a broad representation of design variables affecting shear capacity. By focusing exclusively on experimentally validated data rather than incorporating finite element simulations, this study aims to eliminate uncertainties associated with numerical modeling assumptions. This approach ensures a reliable and unbiased basis for training ML models capable of accurately predicting the shear strength, with key influencing variables include:

- Concrete CS (f'_c, MPa): Ranges from 19.62 to 132.10 MPa with a mean value of 52.21 MPa.
- Shear span-to-depth ratio (a/H): Ranges from 0.27 to 2.00, with a mean value of 0.94.
- Opening size ratios (a_x/a, a_y/a): Represent the relative dimensions of openings in the web, influencing the structural behavior.
- Opening location ratios (X_0/a, Y_0/H): Define the positioning of openings, which affects stress distribution and failure mechanisms.
- Reinforcement yield strength (f_y, MPa): Varies significantly, ranging from 0 MPa to 820 MPa, with an average of 495.81 MPa.
- Web reinforcement ratios (ρ_{sw}, ρ_s, %): Include horizontal and vertical reinforcement ratios, contributing to shear resistance.
- Shear strength (V, kN): The output variable of interest, ranging from 14.00 kN to 1248.14 kN, with a mean value of 289.87 kN.

Table 1. Information of the features used

	Mean	Std	Min	Q25	Q50	Q75	Max
Input							
Concrete CS – f'_c (MPa)	52.21	24.95	19.62	27.00	52.90	73.00	132.10
Shear span-to-depth ratio – a/H	0.93	0.48	0.27	0.50	0.90	1.50	2.00
Opening size - a_x/a	0.37	0.25	0.00	0.17	0.35	0.50	1.50
Opening size - a_y/a	0.23	0.12	0.00	0.13	0.20	0.30	0.63
Opening location - X_0/a	0.34	0.23	0.00	0.25	0.31	0.41	1.66
Opening location - Y_0/H	0.36	0.13	0.00	0.33	0.38	0.42	1.00
Reinforcement yield strength - f_y (MPa)	495.81	178.25	0.00	420.00	500.00	562.25	820.00
Horizontal web reinforcement ratio - ρ_{sw} (%)	1.10	0.73	0.00	0.87	1.00	1.02	5.43
Vertical web reinforcement ratio - ρ_s (%)	0.19	0.30	0.00	0.00	0.00	0.42	1.52
Output							
Shear strength - V (kN)	289.87	240.69	14.00	125.14	205.20	383.75	1248.14

Violin plots were utilized in this study to explore the distribution and variability of input and output parameters, providing a detailed visualization of the data's probability density at different values. The width of the plot at any given point reflects the density of the data. Fig. 2 displays violin plots for all input and output parameters, offering insights into their statistical distributions. The symmetrical and elongated shapes of these plots illustrate the spread and clustering of data points. Dashed lines within each violin plot represent the quartiles (Q25, Q50, Q75), which

help to identify central tendencies and potential skewness in the data. For instance, the distribution of shear strength (V) shows a slight right skewness, indicating a predominance of lower-strength beams with fewer high-strength outliers. Similarly, reinforcement yield strength (f_y) exhibits a broader distribution, reflecting the diverse range of reinforcement grades included in the dataset.

This visualization provides an understanding of how different parameters are distributed across the dataset, helping in identifying patterns, variability, and potential outliers that may influence model development and prediction accuracy.

To investigate the relationships between input and output parameters, a correlation analysis was conducted, with the results visualized in a correlation matrix heatmap (Fig. 3). The heatmap uses a color gradient to represent Pearson correlation coefficient, ranging from -1 (strong negative correlation) to 1 (strong positive correlation), with neutral correlations close to 0 depicted in white or light colors. This visualization provides a clear overview of the dependencies among variables.

The analysis highlights several key relationships relevant to the structural behavior of RC deep beams. Parameters such as concrete CS (f'_c), shear span-to-depth ratio (a/H), reinforcement yield strength (f_y), and web reinforcement ratios (ρ_{sw}, ρ_s) exhibit moderate to strong correlations with shear strength (V), validating their inclusion as critical predictors in the model. Furthermore, opening size ratios (a_x/a, a_y/a) and location ratios (X_0/a, Y_0/H) also show significant effects, demonstrating their role in modifying stress distribution and influencing failure mechanisms.

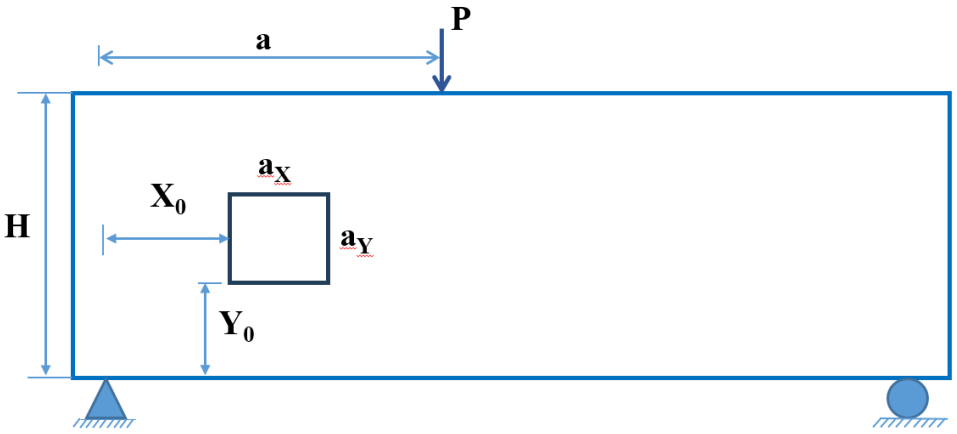

Fig. 1. Geometric parameters of beams

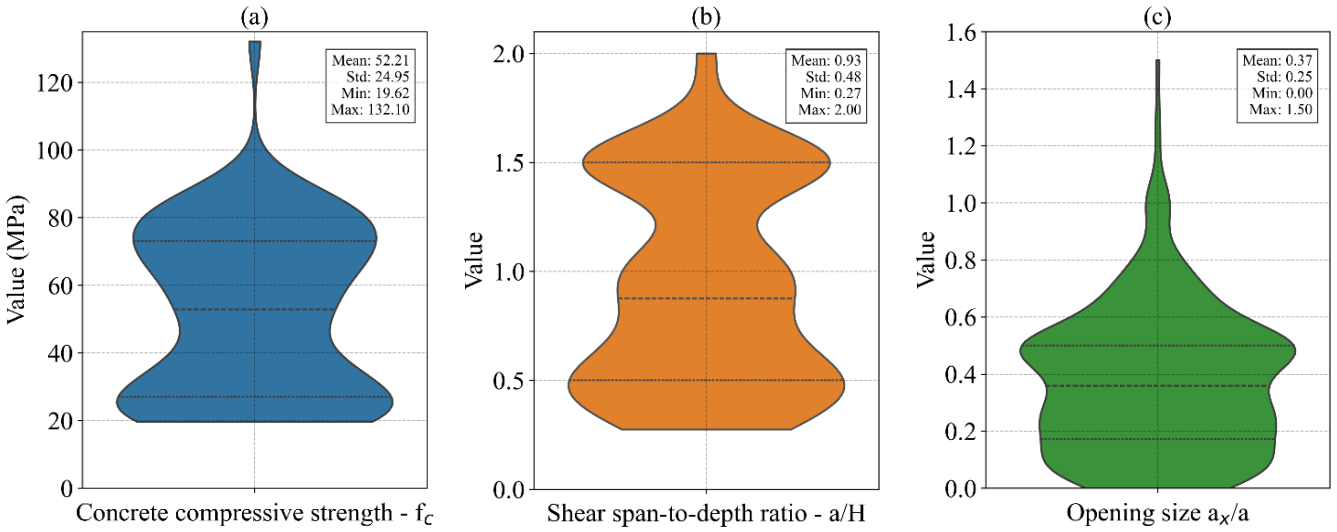

Fig. 2. Violin plots of parameters and shear strength distribution

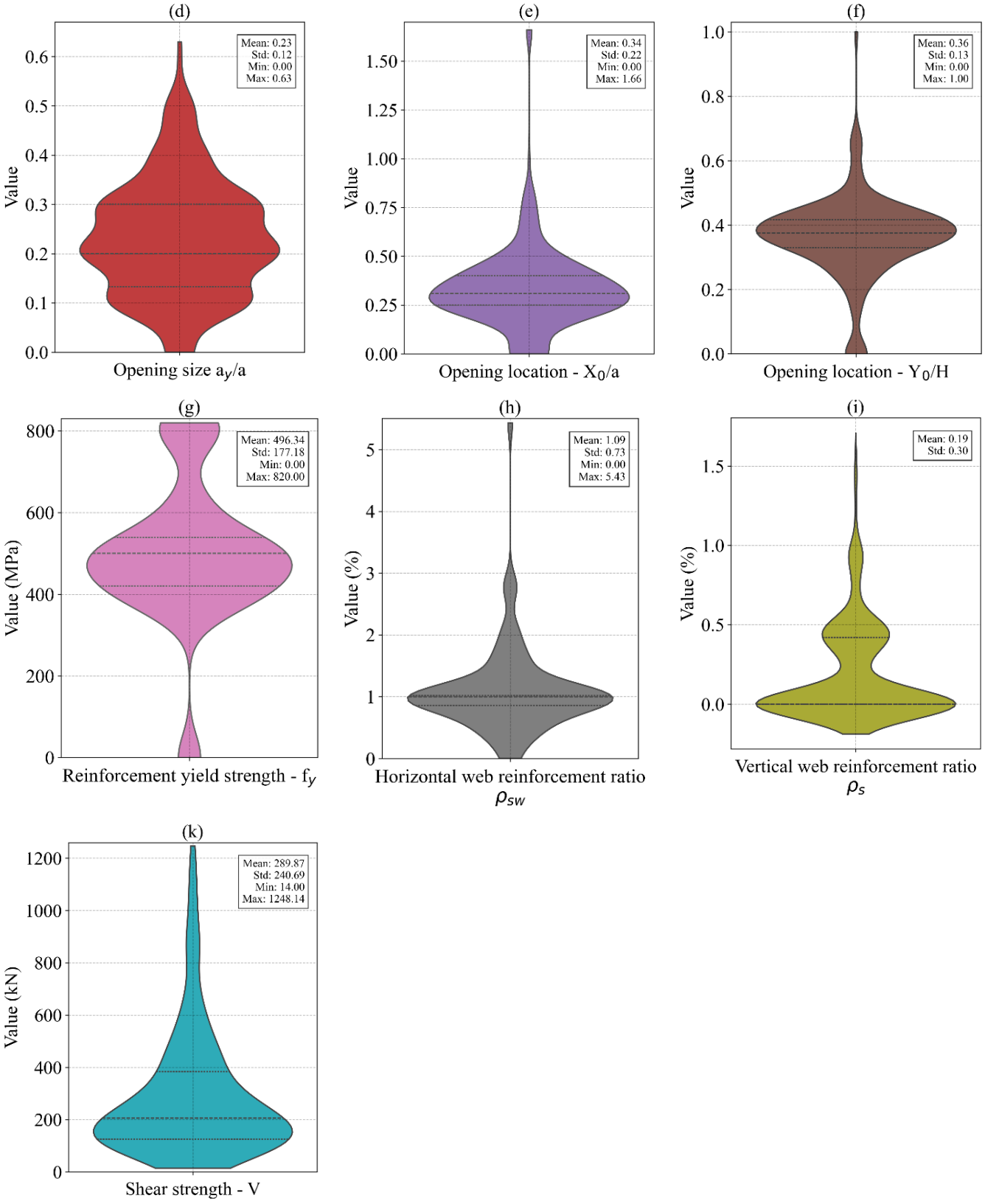

Fig. 2. (continued)

This correlation analysis justifies the selection of nine input variables used in this study, as they comprehensively capture the geometric, material, and reinforcement properties that govern the shear behavior of RC deep beams. The insights gained from this analysis reinforce the importance of these parameters in accurately predicting shear strength.

3. ML Methods

3.1. Gradient Boosting

Gradient Boosting (GB) is an ensemble learning method that builds predictive models iteratively by addressing the residual errors of previously constructed models [39]. This sequential process improves model accuracy by concentrating on instances that are more challenging to predict. The core mechanism of GB involves minimizing a specified loss function using gradient descent optimization. Each successive tree in the ensemble is trained to minimize the errors calculated by earlier trees, thereby enhancing overall predictive performance. A distinguishing feature of GB, compared to traditional boosting methods, is the inclusion of a learning rate parameter. This parameter regulates the contribution of each tree to the final model, helping to prevent overfitting and promoting robust generalization. Due to its ability to effectively model complex nonlinear relationships and interactions among features, GB has been extensively applied across various engineering and scientific fields where accurate predictions are required.

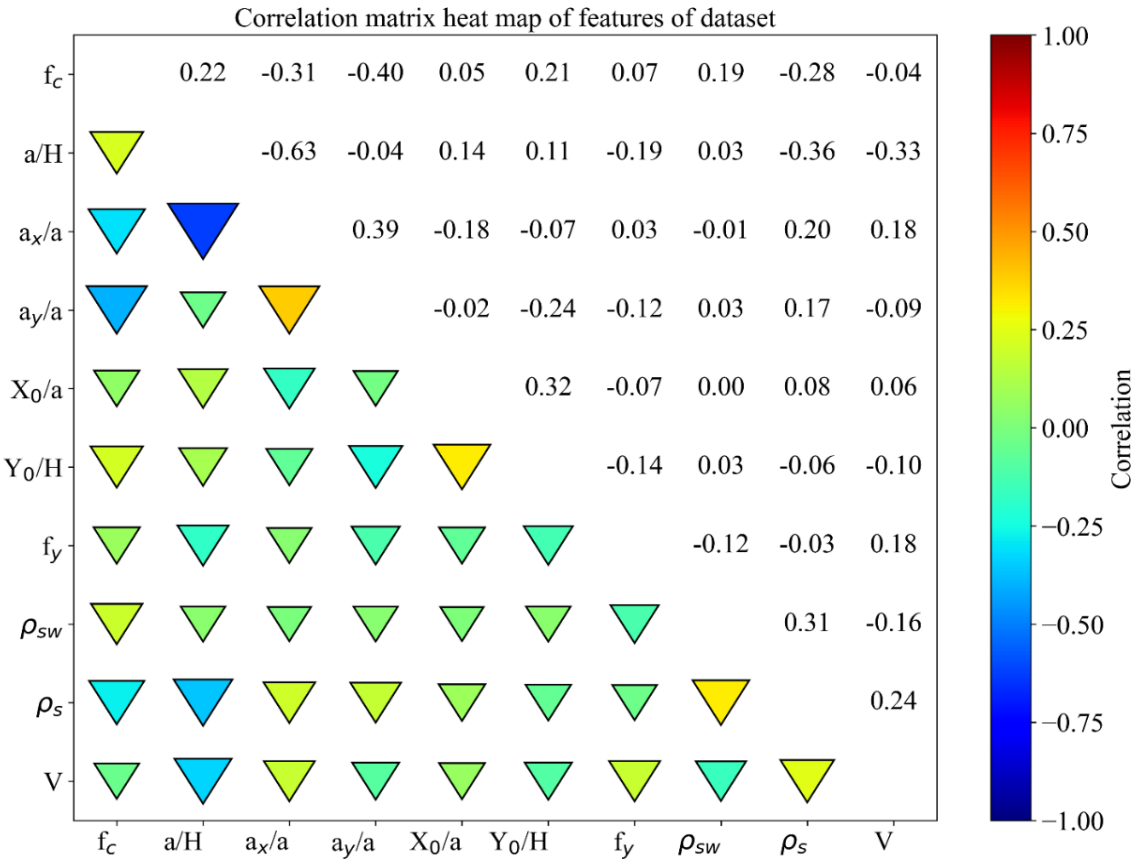

Fig. 3. Correlation matrix between parameters in the dataset

3.2. Hyperparameter Optimization using Metaheuristic Algorithms

a. Golden Jackal Optimization

The GJO algorithm, introduced in 2022 [40], is a nature-inspired metaheuristic optimization method modeled on the cooperative hunting behavior of golden jackals. This behavior, typically involving male and female jackals hunting in pairs, serves as the foundation for simulating the exploration and exploitation processes in optimization problems. The algorithm has been applied to various engineering and computational challenges due to its simplicity, efficiency, and adaptability.

The GJO algorithm consists of three primary phases that mimic the hunting process of golden jackals. In the exploration phase, agents search the solution space for potential prey (solutions), analogous to jackals detecting prey. This is followed by the encirclement phase, where agents

strategically surround and disturb the prey, facilitating convergence toward promising regions of the search space. Finally, the attacking phase intensifies the search around the best solutions identified, ensuring global optimization by refining these solutions further.

By balancing exploration (searching across the solution space) and exploitation (refining promising solutions), GJO demonstrates robust performance across a range of optimization problems. Its biologically inspired mechanisms allow it to effectively address complex optimization tasks while maintaining computational simplicity. However, like many metaheuristic algorithms, GJO can sometimes face challenges such as premature convergence to local optima or insufficient global exploration. To address these limitations, several modified versions of GJO have been proposed, incorporating hybrid strategies or enhancements like differential evolution or Q-learning mechanisms to improve convergence accuracy and global search capabilities.

b. Honey Badger Algorithm

The HBA, introduced in 2022 [41], is a bio-inspired metaheuristic optimization technique modeled on the foraging behavior of honey badgers. Well-known for their problem-solving abilities, honey badgers use scent tracking and strategic digging to locate food, behaviors that are emulated in HBA to balance exploration and exploitation effectively during the optimization process.

HBA operates through two primary phases: the Digging Phase and the Honey Phase. In the former, the algorithm mimics the honey badger's random exploration, where individuals dynamically search the solution space guided by scent trails. This phase ensures broad exploration, reducing the likelihood of premature convergence to local optima. In the latter phase, the search intensifies around promising regions, similar to how honey badgers focus on beehives. During this phase, individuals refine their positions based on environmental feedback, converging toward optimal solutions.

The algorithm incorporates mechanisms such as a smell intensity parameter to guide movement and a density factor to transition smoothly between exploration and exploitation. These features enable HBA to adapt dynamically throughout the search process. Its simplicity, requiring few control parameters, and its ability to balance global exploration with local refinement make it a competitive alternative for solving complex optimization problems. HBA has demonstrated robust performance across various benchmark tests and real-world applications, including engineering design and statistical modeling, due to its efficient convergence properties and adaptability.

3.3. Model performance evaluation

To assess the performance of the optimized GB model, several metrics are utilized to comprehensively evaluate predictive accuracy and facilitate comparisons across different model configurations. These metrics include mean absolute error (MAE), root mean squared error (RMSE), coefficient of determination (R^2), and mean absolute percentage error. These metrics can be found in the literature and calculated using the following:

$$R^2=1-\frac{\sum_{i=1}^{n}\left(Ac_i-Pr_i\right)^2}{\sum_{i=1}^{N}\left(Ac_i-\overline{Ac}\right)^2} \quad (1)$$

$$RMSE=\sqrt{\frac{1}{n}\sum_{i=1}^{n}\left(Ac_i-Pr_i\right)^2} \quad (2)$$

$$MAE=\frac{1}{n}\sum_{i=1}^{n}\left|Ac_i-Pr_i\right| \quad (3)$$

$$MAPE=\frac{1}{n}\sum_{i=1}^{n}\frac{\left|Ac_i-Pr_i\right|}{Ac_i}\times 100\% \quad (4)$$

where n is the number of samples, Ac_i is the actual value, Pr_i is the predicted value, and $\overline{Ac}$ is the average of the actual and predicted values.

3.4. Methodological diagram of the study

The methodology for applying the GB model comprises four key stages, as illustrated in Fig. 4.

Step 1: Data compilation and division

A dataset of 314 experimental tests, sourced from 18 peer-reviewed publications, is assembled. This dataset is divided randomly into train dataset and test dataset using a 70/30 split, with 70% allocated for training and 30% for testing.

Step 2: Hyperparameter optimization

Two metaheuristic algorithms, GJO and HBA, are utilized to optimize five key hyperparameters of the GB model. Each algorithm is tested with population sizes of 10, 20, and 30, aiming to maximize the coefficient of determination (R^2) across both train and test datasets.

Step 3: Model selection

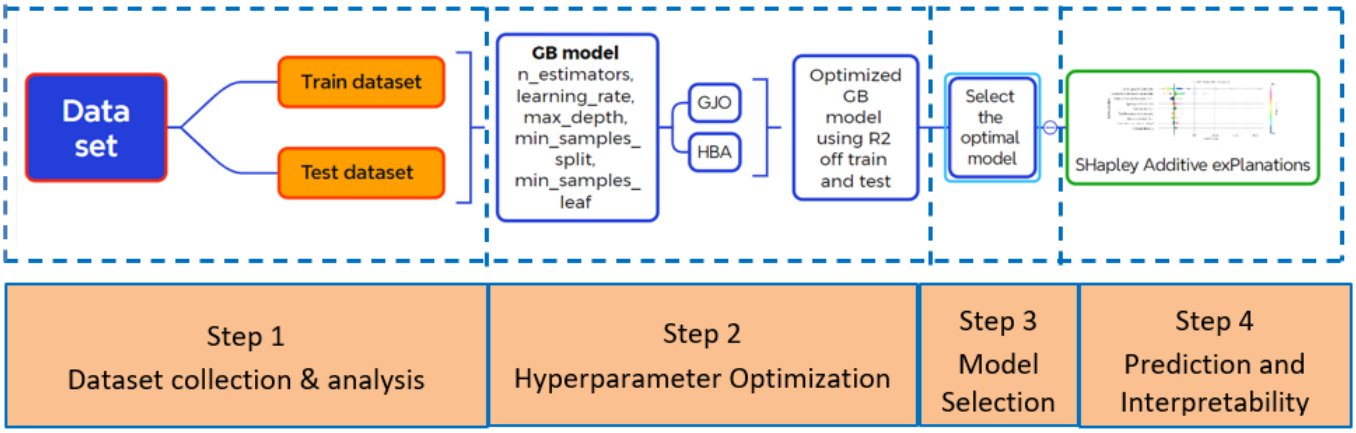

Fig. 4. Methodological diagram of the study

The performance of the six optimized GB models (GB_01 to GB_06) is evaluated based on their R^2 values. The model exhibiting the highest R^2 on the test dataset is selected as the optimal model. Additionally, to ensure the robustness of the selected hyperparameters, a Monte Carlo (MC) stability analysis was performed. The optimized model (GB_06) was retrained and evaluated 500 times on different random 70/30 data splits to confirm that its performance is not an artifact of a single data partition.

Step 4: Prediction and interpretability analysis

The selected model is used to predict the shear strength of RC deep beams with web openings. Additionally, SHAP values are employed to enhance the interpretability of the model by analyzing the contribution of each input feature to the predictions.

4. Results and Discussion

4.1. Hyperparameter Optimization of GB Model

Hyperparameter optimization is critical for improving the performance of ML models, particularly for complex ensemble methods such as GB. Proper selection of hyperparameter values directly influences the model's ability to generalize, its computational efficiency, and its predictive accuracy. Without effective tuning, the model risks overfitting or underfitting, which can result in suboptimal performance on unseen data.

In this study, five key hyperparameters of the GB model were optimized to achieve improved performance. The number of estimators (n_estimators), which determines the number of boosting iterations, was explored within a range of 1 to 500. The learning rate (learning_rate), a parameter that balances convergence speed and model stability, was tuned within the range of 0.01 to 0.3. To control the complexity of individual base learners and prevent overfitting, the max_depth was set between 1 and 8. Additionally, the minimum samples required to split an internal node (min_samples_split) was varied within 2 to 10, ensuring sufficient data per split to maintain model stability. The minimum samples required for a leaf node (min_samples_leaf) was also tuned within the range of 1 to 10 to regulate tree growth and mitigate overfitting.

To optimize these hyperparameters, two nature-inspired metaheuristic algorithms were

employed: GJO and the HBA. These population-based search methods iteratively explored the hyperparameter space to identify configurations that maximized the R^2 on both training and testing datasets. By leveraging these advanced optimization techniques, the study ensured that the GB model achieved a balance between predictive accuracy and generalization capability.

To evaluate the impact of population size (Pop_size) on optimization effectiveness, both the GJO and HBA were executed with three population sizes: 10, 20, and 30. These values were chosen to systematically evaluate the trade-off between optimization thoroughness and computational expense, aligning with recommendations in [41–43] for efficient convergence in engineering applications. This variation allowed for a detailed analysis of how population size influences convergence behavior and final model performance. Consequently, six GB models (GB_01 to GB_06) were developed, each corresponding to a unique combination of optimization algorithm and population size.

The optimization process, as illustrated in Fig. 5, demonstrates the evolution of R^2 values over iterations for different population sizes under both algorithms. Both GJO and HBA achieved high R^2 values, with GJO slightly outperforming HBA in terms of final predictive accuracy. Table 2 summarizes the R^2 values for training and testing datasets alongside the total runtime for each model. The results indicate that all models achieved excellent predictive performance, with R^2 values exceeding 0.9600 across both datasets.

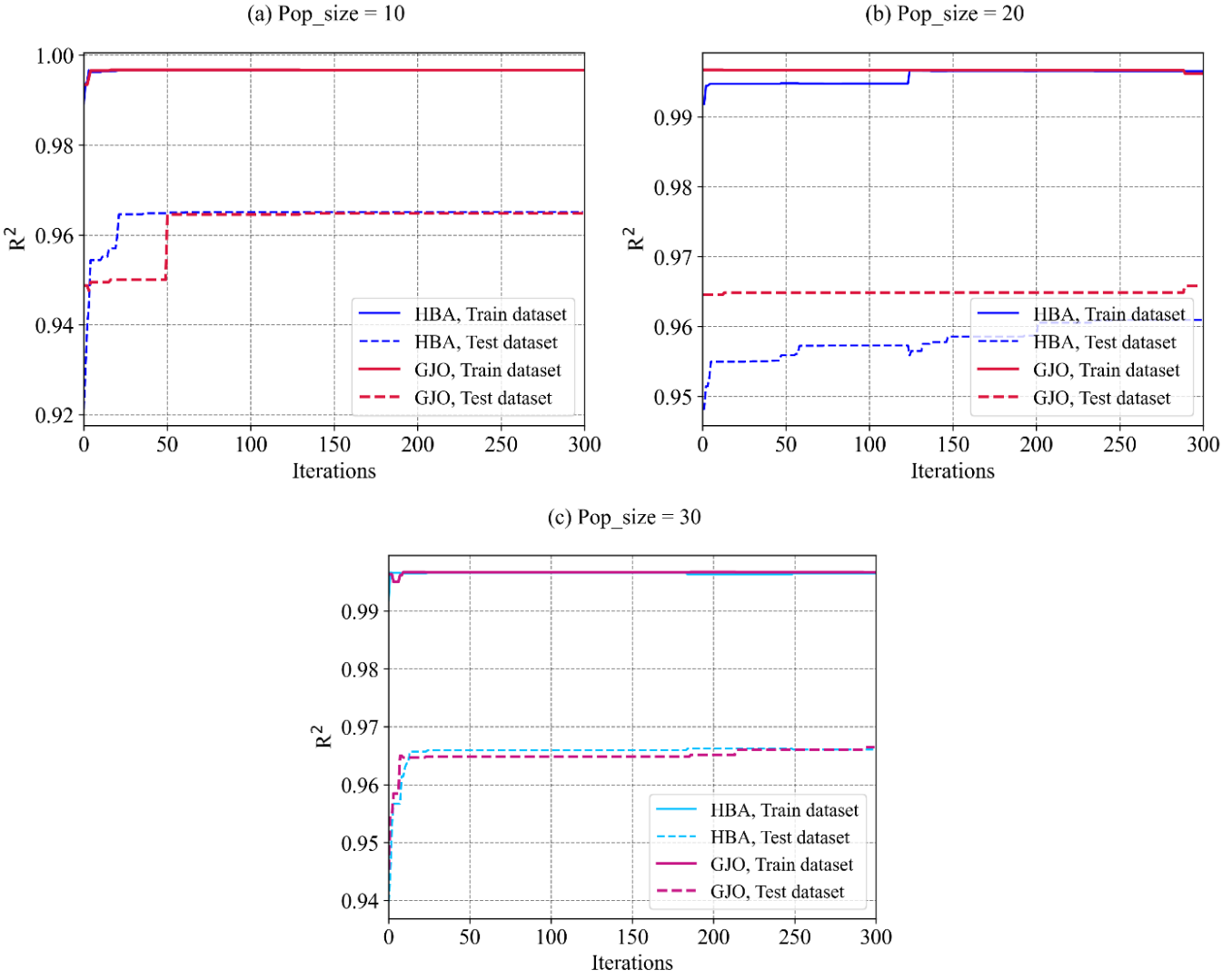

Fig. 5. R^2 values for train dataset and test dataset for HBA and GJO optimization algorithms

Table 2. Comparison of performance of GB models optimized by HBA and GJO with different population sizes

Model	Optimization Algorithm	R^2_train	R^2_test	Run total (s)
GB_01	HBA, Pop_size = 10	0.9966	0.9651	1399.13
GB_02	GJO, Pop_size = 10	0.9967	0.9648	1451.48
GB_03	HBA, Pop_size = 20	0.9965	0.9609	1689.91
GB_04	GJO, Pop_size = 20	0.9962	0.9658	2272.67
GB_05	HBA, Pop_size = 30	0.9965	0.9661	3790.39
GB_06	GJO, Pop_size = 30	0.9967	0.9664	2927.91

It was observed that increasing population size consistently enhanced model accuracy, as evidenced by improved R^2 values from Pop_size = 10 to 30. Among all models, GB_06 (GJO with Pop_size = 30) exhibited the highest test dataset R^2 value (0.9664), indicating superior generalization performance. Although GB_06 did not achieve the shortest runtime (2927.91 seconds), it was more computationally efficient compared to GB_05 (HBA with Pop_size = 30), which required a longer runtime of 3790.39 seconds.

Given its balance between predictive accuracy and computational efficiency, GB_06 was selected as the representative model for further analysis and presentation of results. This selection underscores the importance of optimizing population size to achieve a trade-off between convergence speed and final model performance in metaheuristic-based optimization processes.

4.2. Stability analysis via Monte Carlo simulation

To evaluate the stability of the model's performance with the optimized hyperparameters, 500 independent MC simulations were conducted. This analysis aimed to ensure that the model's high performance was not an artifact of a single, specific train-test split but rather a generalizable characteristic of the optimized parameter set. In each simulation, the entire dataset of 314 samples underwent random re-shuffling and was partitioned into new 70% train and 30% test datasets. The GB_06 model, utilizing the same set of optimized hyperparameters identified, was trained on each new train dataset and evaluated on the corresponding test dataset. The normalized convergence of the RMSE and the (R^2 over the 500 simulations is presented in Fig. 6.

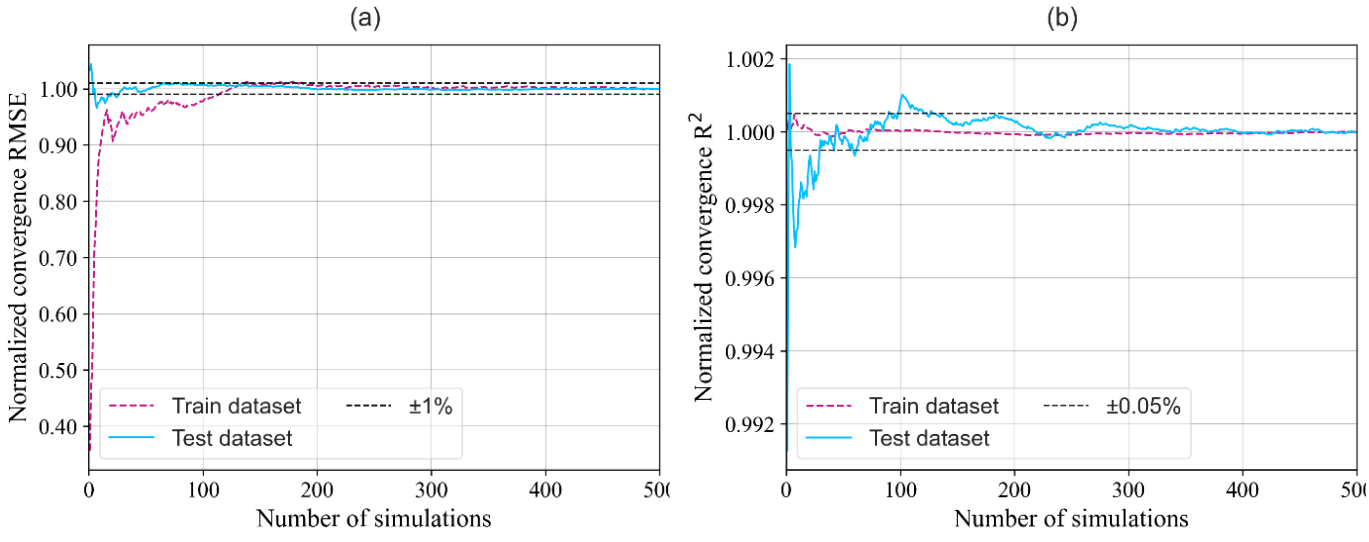

Fig. 6. Normalized convergence plots for (a) RMSE and (b) R^2 over 500 MC simulations

The results show stability, particularly for the test dataset. As seen in Fig. 6b, the R^2 value rapidly converges and remains within a very narrow tolerance of ±0.05%. Similarly, Fig. 6a shows that the RMSE for the test set converges stably within a ±1% band. This high degree of stability across numerous random data partitions evidence that the chosen hyperparameters are stable and the model generalizes well. The analysis confirms that the predictive performance is a reliable characteristic of the model and is not sensitive to the particular composition of the train dataset.

4.3. Representative prediction results

Following the successful stability validation of the GB_06 hyperparameters, the predictive capabilities of this representative model were analyzed in detail. To analyze the predictive capabilities of the optimized GB model (GB_06), a combination of statistical evaluations and graphical interpretations was employed, with its performance compared to a baseline GB model (GB_default) trained using default hyperparameters. Table 3 provides a summary of the performance metrics, while Figs. 7 and 8 illustrate error distributions and regression plots, respectively.

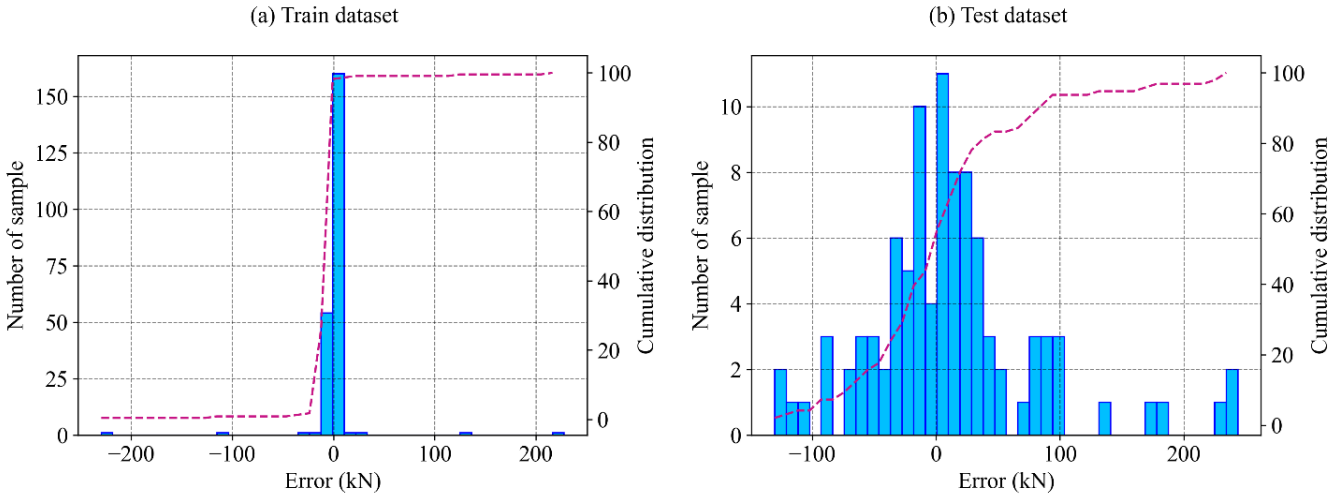

Fig. 7. Error between the SS prediction results and actual values for different datasets: (a) train, (b) test

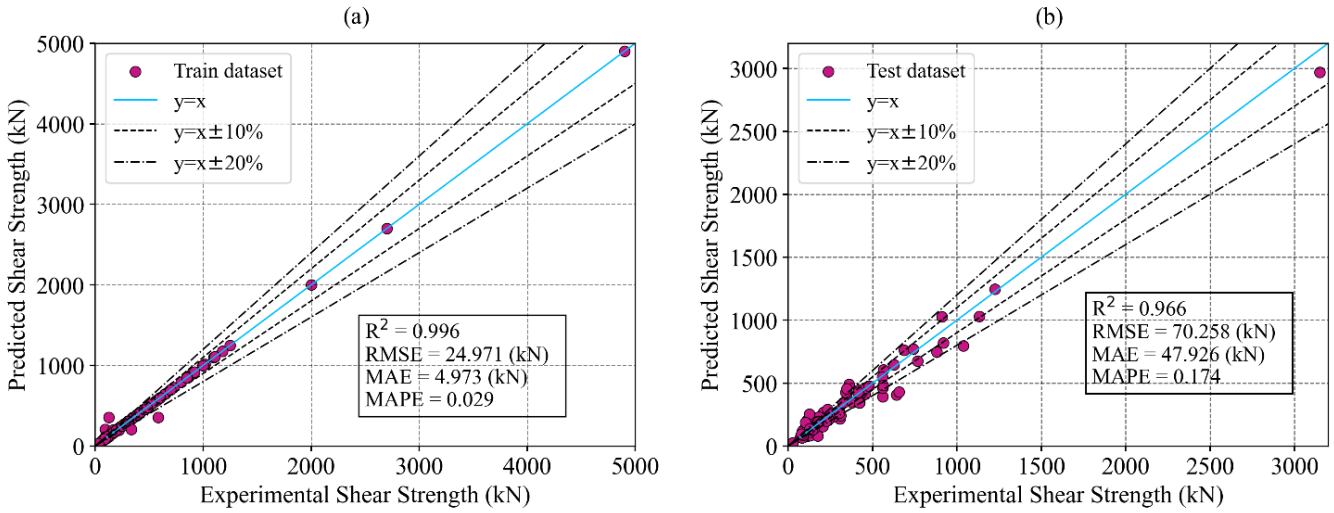

Fig. 8. Regression charts between SS prediction results and actual values for different datasets: (a) train, (b) test

Fig. 7a shows the error distribution for GB_06 on the training dataset, represented as a histogram with a narrow peak centered around 0 kN. Most prediction errors fall within ±5 kN, with a standard deviation of approximately 2.5 kN, indicating high precision and effective pattern capture in the

training data. Fig. 7b depicts the test dataset error distribution, which is slightly broader, with errors ranging from -20 kN to 20 kN and a standard deviation of about 4 kN. Despite this broader range, the distribution remains centered around zero, aligning with the inherent variability in the dataset, where shear strength values range from 14.00 kN to 1248.14 kN (mean: 289.87 kN). These results demonstrate that GB_06 generalizes well to unseen data.

Fig. 8 displays regression plots for both datasets, highlighting the strong correlation between predicted and actual shear strength values for GB_06. The points closely follow the diagonal line, further confirming the model's predictive accuracy.

Table 3. Typical prediction results of GB model

Dataset	RMSE (kN)	MAE (kN)	R^2	MAPE
Model GB_06				
Train	24.871	4.973	0.996	0.029
Test	70.258	47.962	0.966	0.174
All	43.841	17.940	0.989	0.073
Model GB_default				
Train	52.880	36.262	0.985	0.167
Test	102.835	61.349	0.928	0.322
All	71.726	43.835	0.970	0.214

Quantitative metrics in Table 3 reveal that GB_06 outperforms GB_default across all evaluation criteria. On the test dataset, GB_06 achieves an R^2 value of 0.9664, MAE of 47.962 kN, and RMSE of 70.258 kN. In comparison, GB_default records an R^2 of 0.928, an MAE of 61.349 kN, and an RMSE of 102.835 kN. Notably, GB_06 achieves a 31.68% reduction in RMSE and a 21.82% reduction in MAE compared to GB_default, underscoring the effectiveness of GJO-based hyperparameter tuning in enhancing model accuracy.

Overall, these results confirm that GB_06 provides superior predictive performance while maintaining robust generalization capabilities, making it a reliable tool for predicting shear strength in RC deep beams with web openings.

4.4. Analysis of feature contributions to shear strength using SHAP values

An analysis of feature importance was conducted using SHAP (SHapley Additive exPlanations) values to examine the factors influencing the shear strength (V) of RC deep beams with web openings, based on the optimized GB model (GB_06). SHAP values were calculated to quantify the contribution of each input feature to the model's predictions, capturing both linear and nonlinear relationships. The results are presented in Fig. 9, which includes two visualizations: a Bee-Swarm SHAP plot (Fig. 9a) and a bar chart of mean absolute SHAP values (Fig. 9b).

In Fig. 9a, individual SHAP values are depicted as dots, with their colors indicating feature magnitudes (red for higher values and blue for lower values). The x-axis reflects the variability in feature influence on shear strength predictions. The shear span-to-depth ratio (a/H) exhibits the broadest range of SHAP values, signifying its substantial and variable impact on shear strength, consistent with its structural importance in deep beams [44].

The horizontal web reinforcement ratio (ρ_{sw}) predominantly exhibits positive SHAP values (red dots for higher reinforcement levels) in the bee-swarm plot (Fig. 9a), indicating that increased horizontal reinforcement generally enhances shear resistance by mitigating shear-induced cracking around web openings, consistent with findings in [5, 9, 22]. However, some red dots with negative SHAP values reflect cases where large openings

or suboptimal locations reduce shear strength. Additionally, green dots (lower ρ_{sw} values) on the positive side suggest that low reinforcement levels can still contribute to shear strength when supported by other factors, such as high concrete compressive strength or favorable geometry.

Conversely, the opening size ratio (a_x/a) displays mixed positive and negative SHAP values; smaller openings (blue dots) are often associated with improved shear strength due to reduced stress concentrations. Similarly, the opening location ratio (Y_0/H) reveals that higher positions tend to reduce shear strength, likely due to proximity to critical shear zones affecting load transfer mechanisms.

Fig. 9b ranks features based on their mean absolute SHAP values. The shear span-to-depth ratio (a/H) emerges as the most influential parameter (mean absolute SHAP value: 153.07), followed by ρ_{sw} (93.52) and the vertical web reinforcement ratio (ρ_s) (51.41). Other features include Y_0/H (27.86), a_y/a (25.1), X_0/a (21.1), f_y (21.23), f'_c (19.96), and a_x/a (17.63). The relatively lower ranking of concrete CS (f'_c) suggests that its effect on shear strength is more dependent on interactions with other features rather than being a dominant factor independently.

These findings affirm that parameters such as shear span-to-depth ratio, web reinforcement ratios, and opening characteristics are primary determinants of shear strength in RC deep beams with web openings. This analysis provides valuable insights for refining design methodologies and improving structural modeling approaches in engineering applications.

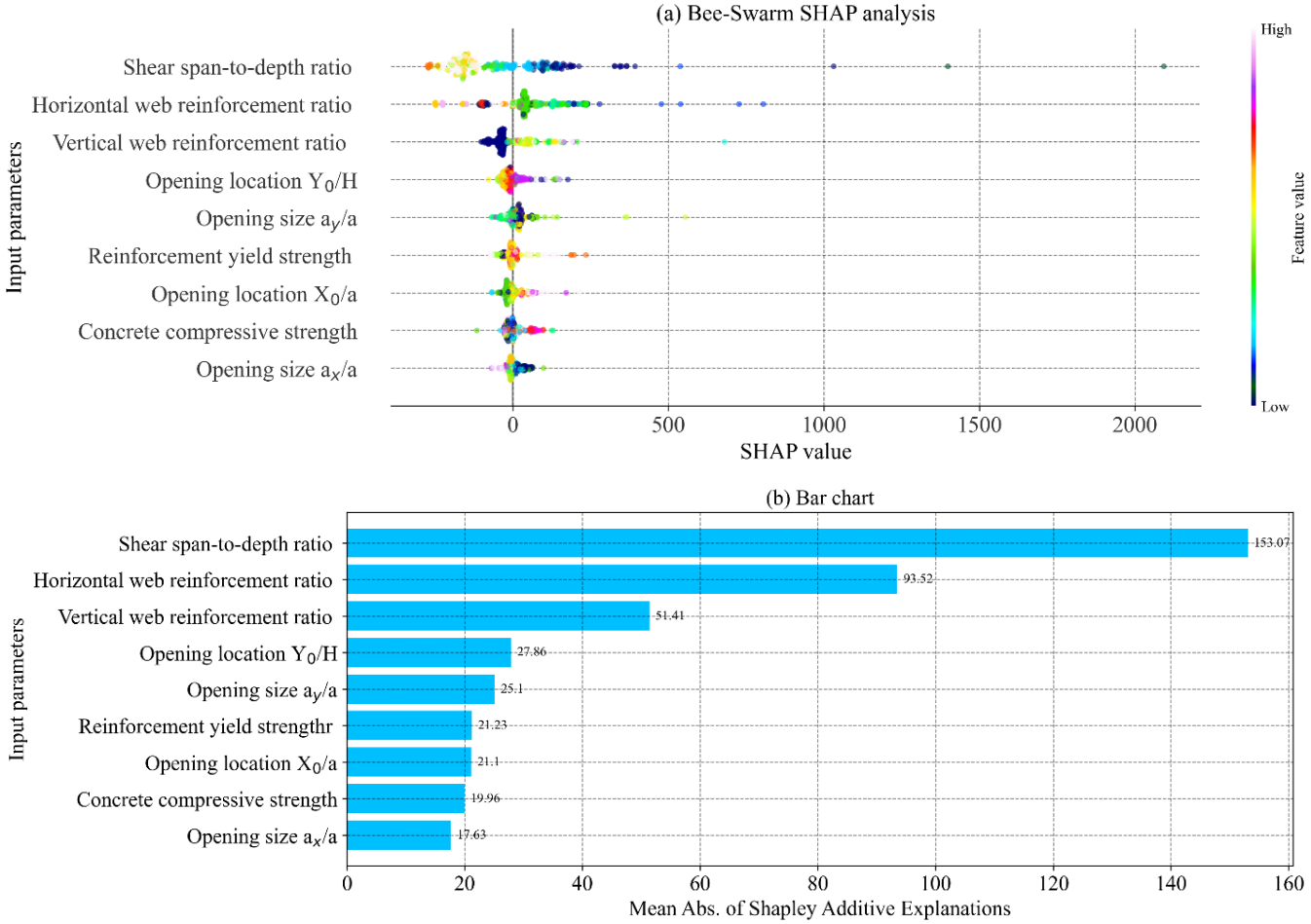

Fig. 9. SHAP-Based feature importance analysis for shear strength prediction in RC deep beams

5. Conclusion

An optimized GB model was developed and validated to predict the shear strength of RC deep beams with web openings, addressing challenges inherent in traditional empirical and analytical methods. The model was trained using a dataset of

314 experimentally tested beams sourced from peer-reviewed publications, ensuring a robust basis for analysis. Hyperparameter optimization was conducted using two metaheuristic algorithms: GJO and HBA. Among the models developed, the GJO-optimized version, designated as GB_06, demonstrated superior performance, achieving an R^2 value of 0.9664 and a RMSE of 70.258 kN on the test dataset. Superior performance was achieved relative to the baseline GB model with default hyperparameters (R^2 = 0.928, RMSE = 102.835 kN), indicating the effectiveness of metaheuristic optimization techniques for improving predictive accuracy. Furthermore, the model's stability was rigorously confirmed through a 500-run MC simulation, which demonstrated that the high R^2 and low RMSE values are robust and not dependent on a specific data split.

Feature importance analysis, conducted using SHAP values, identified the shear span-to-depth ratio (a/H), horizontal web reinforcement ratio (ρ_{sw}), and vertical web reinforcement ratio (ρ_s) as the most influential factors affecting shear strength predictions. These results are consistent with established principles in structural mechanics, highlighting the critical role of these parameters in governing the behavior of RC deep beams with web openings.

The optimized GB model's ability to capture complex nonlinear relationships provides a reliable alternative to costly and time-intensive experimental testing. More specifically, this model offers significant practical benefits for structural engineers. It serves as an efficient design support tool, enabling rapid and accurate prediction of shear strength. Engineers can leverage the model to perform parametric studies - for instance, varying the size and location of openings or reinforcement ratios - to identify optimal design solutions or to rapidly assess the safety of existing structures. Furthermore, the use of SHAP analysis bridges the "black-box" gap, allowing engineers to understand the key factors driving the predictions. This offers practical benefits for improving design efficiency and ensuring structural safety in engineering applications.

Reference

[1] K. Mohamed, A.S. Farghaly, B. Benmokrane, K.W. Neale. (2017). Nonlinear finite-element analysis for the behavior prediction and strut efficiency factor of GFRP-reinforced concrete deep beams. *Engineering Structures*, 137, 145-161.https://doi.org/10.1016/j.engstruct.2017.01.045

[2] M.A. Mansur. (1998). Effect of openings on the behaviour and strength of R/C beams in shear. *Cement and Concrete Composites*, 20(6), 477-486. https://doi.org/10.1016/S0958-9465(98)00030-4

[3] X.F. Nie, S.S. Zhang, J.G. Teng, G.M. Chen. (2018). Experimental study on RC T-section beams with an FRP-strengthened web opening. *Composite Structures*, 185, 273-285. https://doi.org/10.1016/j.compstruct.2017.11.018

[4] T. Almusallam, Y. Al-Salloum, H. Elsanadedy, A. Alshenawy, R. Iqbal. (2018). Behavior of FRP-Strengthened RC Beams with Large Rectangular Web Openings in Flexure Zones: Experimental and Numerical Study. *International Journal of Concrete Structures and Materials*, 12, 47. https://doi.org/10.1186/s40069-018-0272-5

[5] G. Campione, G. Minafò. (2012). Behaviour of concrete deep beams with openings and low shear span-to-depth ratio. *Engineering Structures*, 41, 294-306. https://doi.org/10.1016/j.engstruct.2012.03.055

[6] M.S. Al-Enezi, A.M. Yousef, A.M. Tahwia. (2023). Shear capacity of UHPFRC deep beams with web openings. *Case Studies in Construction Materials*, 18, e02105. https://doi.org/10.1016/j.cscm.2023.e02105

[7] American Concrete Institute. An ACI Standard and Report. (2014). Building Code Requirements for Structural Concrete (ACI 318-14).

[8] AS3600-2018, Concrete Structures. (2018).

Sydney: Standards Australia limited.

[9] K.-H. Yang, H.-S. Chung, A.F. Ashour. (2007). Influence of inclined web reinforcement on reinforced concrete deep beams with web openings. *ACI Structural Journal*, 104(5), 580-589. https://doi.org/10.14359/18860

[10] A. Ashour, K.-H. Yang. (2008). Application of plasticity theory to reinforced concrete deep beams: a review. *Magazine of Concrete Research*, 60(9), 657-664. https://doi.org/10.1680/macr.2008.00038

[11] F.K. Kong, G.R. Sharp, S.C. Appleton, C.J. Beaumont, L.A. Kubik. (1978). Structural idealization for deep beams with web openings: further evidence. *Magazine of Concrete Research*, 30(103), 89-95. https://doi.org/10.1680/macr.1978.30.103.89

[12] L. Kubik. (1980). Predicting the strength of reinforced concrete deep beams with web openings. *Proceedings of the Institution of Civil Engineers*, 69(4), 939. https://doi.org/10.1680/iicep.1980.2178

[13] K.H. Tan, K. Tong, C.Y. Tang. (2003). Consistent strut-and-tie modelling of deep beams with web openings. *Magazine of Concrete Research*, 55(1), 65-75. https://doi.org/10.1680/macr.2003.55.1.65

[14] H.-B. Ly. (2025). Enhanced Predictive Modeling and Insights into Geopolymer Concrete Compressive Strength Prediction. *Journal of Testing and Evaluation*, 53(4). https://doi.org/10.1520/JTE20230808

[15] H.-G.T. Hoang, H.-L. Nguyen, T.-A. Nguyen, H.-B. Ly. (2025). Hybrid machine learning approach for prediction and design optimization of marshall stability in graphene oxide-modified asphalt concrete. *Environmental Research*, 285(Part 5), 122646. https://doi.org/10.1016/j.envres.2025.122646

[16] Q.-B. Vo, X.-N.V. Dao, N.T. Nguyen, T.-H.T. Nguyen, H.-B. Ly. (2024). Assessing the applicability of international AI practices in construction management: A systematic review with implications for Vietnam. *Journal of Science and Transport Technology*, 4(4), 71-94. https://doi.org/10.58845/jstt.utt.2024.en.4.4.71-94

[17] T.-A. Nguyen, M.H. Nguyen, H.-B. Ly. (2024). Unified machine learning approach for predicting CFST column axial load capacity. *Innovative Infrastructure Solutions*, 9, 295. https://doi.org/10.1007/s41062-024-01593-4

[18] M. Saleh, M. AlHamaydeh, M. Zakaria. (2023). Shear capacity prediction for reinforced concrete deep beams with web openings using artificial intelligence methods. *Engineering Structures*, 280,115675. https://doi.org/10.1016/j.engstruct.2023.115675

[19] K. Megahed. (2024). Prediction and reliability analysis of shear strength of RC deep beams. *Scientific Reports*, 14, 14590. https://doi.org/10.1038/s41598-024-64386-w

[20] D.S. Augustino. (2024). Shear Performance of Deep Concrete Beams with Openings Using Waste Tyre Steel Fibres: FEM and ANN Analysis. *Civil Engineering Journal*, 10(8), 2422-2449. https://doi.org/10.28991/CEJ-2024-010-08-02

[21] M.V. Chien. (2024). Predicting the shear strength of FRP-RC beams using optimized CatBoost machine learning model (Vietnamese). *Journal of Science and Transport Technology*, 4(3), 13-27. https://doi.org/10.58845/jstt.utt.2024.vn.4.3.13-27

[22] W.-Y. Lu, G.-Z. Lin, C.-C. Tseng, S.-J. Lin. (2020). Shear strength of reinforced concrete deep beams with web openings. *Journal of the Chinese Institute of Engineers*, 43(7), 694-705. https://doi.org/10.1080/02533839.2020.1796816

[23] T.-M. Yoo, J.-H. Doh, H. Guan, S. Fragomeni. (2013). Experimental behaviour of high-strength concrete deep beams with web openings. *The Structural Design of Tall and Special Buildings*, 22(8), 655-676. https://doi.org/10.1002/tal.718

[24] Q. Hussain, A. Pimanmas. (2015). Shear strengthening of RC deep beams with openings using sprayed glass fiber reinforced polymer composites (SGFRP): Part 1. Experimental study. *KSCE Journal of Civil Engineering*, 19(7), 2121-2133. https://doi.org/10.1007/s12205-015-0243-1

[25] K.S. Abdul-Razzaq, H.I. Ali, M.M. Abdul-Kareem. (2018). A new strengthening technique for deep beam openings using steel plates. *International Journal of Applied Engineering Research*, 12(24), 15935-15947.

[26] T. El Maaddawy, S. Sherif. (2009). FRP composites for shear strengthening of reinforced concrete deep beams with openings. *Composite Structures*, 89(1), 60-69. https://doi.org/10.1016/j.compstruct.2008.06.022

[27] W.A. Jasim, A.A. Allawi, N.K. Oukaili. (2018). Strength and serviceability of reinforced concrete deep beams with large web openings created in shear spans. *Civil Engineering Journal*, 4(11), 2560-2574. https://doi.org/10.28991/cej-03091181

[28] W.A. Jasim, Y.B.A. Tahnat, A.M. Halahla. (2020). Behavior of reinforced concrete deep beam with web openings strengthened with (CFRP) sheet. *Structures*, 26, 785-800. https://doi.org/10.1016/j.istruc.2020.05.003

[29] O.E. Hu, K.H. Tan. (2007). Large reinforced-concrete deep beams with web openings: test and strut-and-tie results. *Magazine of Concrete Research*, 59(6), 423-434. https://doi.org/10.1680/macr.2007.59.6.423

[30] I.A.S. Al-Shaarbaf, A.S. Ali, A.J. Abdulridha. (2017). Experimental and numerical investigation of high strength reinforced concrete deep beams with web openings under repeated loading. *Al-Nahrain Journal for Engineering Sciences*, 20(2), 311-325.

[31] A.-H.A. Khalil, E.E. Etman, A.E.A. EL-Nasr. (2004). Behavior of high strength concrete deep beams with openings. *Conference: Scientific Bulletin of Ain Shams University*.

[32] N. Nair, P.E. Kavitha. (2015). Effect of openings in deep beams using strut and tie model method. *International Journal of Technical Research and Applications*, 3(5), 59-62.

[33] H.-C. Eun, Y.-H. Lee, H.-S. Chung, K.-H. Yang. (2006). On the shear strength of reinforced concrete deep beam with web opening. *The Structural Design of Tall and Special Buildings*, 15(4), 445-466. https://doi.org/10.1002/tal.306

[34] I.G. Shaaban, A.H. Zaher, M. Said, W. Montaser, M. Ramadan, G.N. Abd Elhameed. (2020). Effect of partial replacement of coarse aggregate by polystyrene balls on the shear behaviour of deep beams with web openings. *Case Studies in Construction Materials*, 12, e00328. https://doi.org/10.1016/j.cscm.2019.e00328

[35] M.A. Farouk, A.M.R. Moubarak, A. Ibrahim, H. Elwardany. (2023). New alternative techniques for strengthening deep beams with circular and rectangular openings. *Case Studies in Construction Materials*, 19, e02288. https://doi.org/10.1016/j.cscm.2023.e02288

[36] K.-H. Yang, H.-C. Eun, H.-S. Chung. (2003). Effect of the Size and Location of a Web Opening on the Shear Behavior of High-Strength Reinforced Concrete Deep Beams (Korean). *Journal of the Korea Concrete Institute*, 15(5), 697-704.

[37] T.M. Yoo. (2011). Strength and behaviour of high strength concrete deep beam with web openings. *Thesis, Griffith School of Engineering*. DOI 10.25904/1912/2866

[38] H.S. Abed, B.J. Al-Sulayfani. (2023). Experimental and analytical investigation on effect of openings in behavior of reinforced concrete deep beam and enhanced by CFRP laminates. *Structures*, 48, 706-716. https://doi.org/10.1016/j.istruc.2023.01.013

[39] J.H. Friedman. (2001). Greedy Function Approximation: A Gradient Boosting Machine.

The Annals of Statistics, 29(5), 1189-1232. https://doi.org/10.1214/aos/1013203451

[40] N. Chopra, M.M. Ansari. (2022). Golden jackal optimization: A novel nature-inspired optimizer for engineering applications. *Expert Systems with Applications*, 198, 116924. https://doi.org/10.1016/j.eswa.2022.116924

[41] F.A. Hashim, E.H. Houssein, K. Hussain, M.S. Mabrouk, W. Al-Atabany. (2022). Honey Badger Algorithm: New metaheuristic algorithm for solving optimization problems. *Mathematics and Computers in Simulation*, 192, 84-110. https://doi.org/10.1016/j.matcom.2021.08.013

[42] M. Elhoseny, M. Abdel-Salam, I.M. El-Hasnony. (2024). An improved multi-strategy Golden Jackal algorithm for real world engineering problems. *Knowledge-Based Systems*, 295, 111725. https://doi.org/10.1016/j.knosys.2024.111725

[43] J. Wang, W. Wang, K. Chau, L. Qiu, X. Hu, H. Zang, D. Xu. (2024). An Improved Golden Jackal Optimization Algorithm Based on Multi-strategy Mixing for Solving Engineering Optimization Problems. *Journal of Bionic Engineering*, 21, 1092-1115. https://doi.org/10.1007/s42235-023-00469-0

[44] K.-H. Yang, H.-C. Eun, H.-S. Chung. (2006). The influence of web openings on the structural behavior of reinforced high-strength concrete deep beams. *Engineering Structures*, 28(13), 1825-1834. https://doi.org/10.1016/j.engstruct.2006.03.021